First publ. in: Journal of Biological Chemistry 268 (1993), 19, pp. 13850-13857

Kinetic Mechanism of D-Amino Acid Oxidases from *Rhodotorula gracilis* and *Trigonopsis variabilis*[*]

Loredano Pollegioni‡, Bernd Langkau§, Wilhelm Tischer¶, Sandro Ghisla§, and Mirella S. Pilone‡||

From the ‡Department of General Physiology and Biochemistry, University of Milano, 20133 Milano, Italy, the §Fakultät für Biologie, Universität Konstanz, D-7747 Konstanz, Federal Republic of Germany, and ¶Boehringer Mannheim GmbH, W-8122 Penzberg, Federal Republic of Germany

The reaction of two D-amino acid oxidases from the yeasts *Rhodotorula gracilis* and *Trigonopsis variabilis* with the substrates alanine and valine in their 2-^{1}H and 2-^{2}H forms was studied employing the stopped-flow spectrophotometric technique. The turnover numbers at infinite substrate and oxygen concentrations were: 20,700/4,250 and 1,730/360 ([2-^{1}H]/[2-^{2}H]alanine and valine, respectively) for the *Rhodotorula* and 3,150/440 and 2,500/520 ([2-^{1}H]/[2-^{2}H]alanine and valine, respectively) for the *Trigonopsis* enzymes. The rates of anaerobic enzyme flavin reduction were 20,100/4,000 and 1,820/350 ([2-^{1}H]/[2-^{2}H]alanine and valine, respectively) for the *Rhodotorula* and 3,470/350 and 2,460/480 ([2-^{1}H]/[2-^{2}H]alanine and valine, respectively) for the *Trigonopsis* enzymes. The isotope effects on enzyme reduction were 5.0 and 5.2 for *Rhodotorula* and 9.9 and 5.1 for *Trigonopsis* D-amino acid oxidases with alanine and valine, respectively. This suggests that the intrinsic isotope effect on rupture of the substrate α–C–H bond can be as high as 10. The rate-determining step corresponds to the enzyme reductive half-reaction in contrast to the mammalian kidney enzyme where it is the product release from oxidized enzyme (Massey, V., and Gibson, Q. H. (1964) *Fed. Proc.* 23, 18–29). Upon anaerobic reaction with substrate, the yeast enzymes do not form the transient long wavelength absorbing species which are characteristic of the mammalian protein. This is due only in part to rapid dissociation of iminoacid product and is ascribed to intrinsic differences between the charge-transfer complexes of reduced enzyme flavin and product of the yeast as compared to the mammalian enzyme. With the *Trigonopsis* enzyme the flavin radical anion appears to be strongly stabilized and can be produced quantitatively.

In the reaction catalyzed by the flavoprotein D-amino-acid oxidase (EC 1.4.3.3, DAAO),[1] the D-amino acid is oxidized to the corresponding α-ketoacid and ammonia and the coenzyme FAD, which is first reduced, is reoxidized by molecular oxygen to yield hydrogen peroxide (Equation 1):

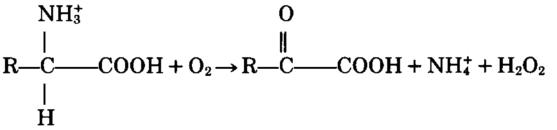

$$R-\underset{H}{\overset{NH_3^+}{C}}-COOH + O_2 \rightarrow R-\overset{O}{\overset{\|}{C}}-COOH + NH_4^+ + H_2O_2 \qquad \text{(Eq. 1)}$$

The kinetic mechanism underlying this overall conversion has been extensively studied in the past for the enzyme purified from pig kidney (PK-DAAO) employing a combination of steady state and stopped-flow kinetic methods (for a review, see Curti *et al.*, 1992). Steady state measurements with D-alanine as substrate indicated a ternary complex mechanism with product release from the oxidized enzyme being the rate-limiting step of the overall reaction (Massey *et al.*, 1961; Massey and Gibson, 1964); the turnover number at infinite substrate concentration was found to be identical to the rate constant for the dissociation of product from the oxidized enzyme complex (Porter *et al.*, 1977). A thorough kinetic analysis of the isotope effects on the reductive half-reaction of PK-DAAO has appeared recently (Denu and Fitzpatrick, 1992).

Steady state measurements with DAAO from *Rhodotorula* and D-alanine as substrate using the oxygen electrode indicated that the kinetic pattern is apparently consistent with a ping pong mechanism; k_{cat} values with D-alanine and D-valine are 43,250 min^{-1} and 31,370 min^{-1}, respectively (Pollegioni *et al.*, 1992a). Kinetic studies for the *Trigonopsis* enzyme (Tv-DAAO) have not yet been reported. The high catalytic efficiency of the *Rhodotorula* enzyme (Rg-DAAO) as compared to PK-DAAO goes along with other peculiar features such as the tight binding of the coenzyme FAD ($K_d = 2.0 \times 10^{-8}$ M) (Casalin *et al.*, 1991), the large value of K_{O_2} (1.77 mM) (Pollegioni *et al.*, 1992a), and differences in the FAD microenvironment (Pollegioni *et al.*, 1992b).

All this taken together indicates that the yeast oxidases shares a common, basic chemical mechanism with PK-DAAO, while the catalytic parameters are significantly different. In the present work we thus address the kinetic mechanism of the Rg- and Tv-DAAOs employing stopped-flow spectrophotometry and using D-alanine and D-valine as substrates in their 2-^{1}H and 2-^{2}H forms, with the goal of defining the differences and similarities. We propose a minimal kinetic scheme for the two yeast enzymes, which involves a ternary complex mechanism, and which is significantly different from that of PK-DAAO with respect to the location of rate-limiting steps. Some mechanistic implications will be discussed.

EXPERIMENTAL PROCEDURES

Glucose oxidase and catalase were purchased from Boehringer and NaBD$_3$CN from Aldrich; α-ketoisovaleric acid and pyruvic acid were

---

[*] This work was supported by Deutsche Forschungsgemeinschaft Grant Gh 2/4-7 (to S. G.) and by grants from Consiglio Nazionale delle Ricerche and Ministero Università Ricerca Scientifica Tenologica (to M. S. P.). The costs of publication of this article were defrayed in part by the payment of page charges. This article must therefore be hereby marked "*advertisement*" in accordance with 18 U.S.C. Section 1734 solely to indicate this fact.

|| To whom correspondence should be addressed: Dept. General Physiology & Biochemistry, 26, via Celoria 20133 Milano, Italy.

[1] The abbreviations used are: DAAO, D-amino acid oxidase; PK-DAAO, D-amino acid oxidase from pig kidney; Tv-DAAO, D-amino acid oxidase from *T. variabilis*; Rg-DAAO, D-amino acid oxidase from *R. gracilis*; AA, amino acid; IA, iminoacid (product of oxidation of the corresponding amino acid).

from Sigma; D-alanine and D-valine were from Merck. All other reagents were of the highest purity commercially available. DAAO from *Trigonopsis variabilis* was furnished by Boehringer Mannheim.

DAAO was purified from *Rhodotorula gracilis* cells (ATCC 26217) following the method of Pollegioni and Pilone (1992c). The ratio A_{274}/A_{455} for pure enzyme was 8.2, and the specific activity on D-alanine as substrate was 180 μmol O_2 min^{-1} mg $protein^{-1}$ at 37 °C; enzyme concentration was determined in terms of flavin content using ϵ_{455} = 12,600 M^{-1} cm^{-1} (Pilone Simonetta *et al.*, 1989a).

Pure DAAO obtained from *T. variabilis* had a ratio A_{274}/A_{450} of about 8.4, an ϵ_{450} = 10,800 M^{-1} cm^{-1} and a specific activity of 37.3 units/mg protein on D-phenylglycine as substrate at 25 °C. It was noted that Tv-DAAO activity progressively decreases during turnover, in particular in the presence of light, and not depending on sensitivity to H_2O_2. This, however, did not have any effect on the experiments reported here, with the exception of reoxidation of free reduced enzyme.

DL-[2-^{2}H]Alanine and DL-[2-^{2}H]valine were prepared as described by Borch *et al.* (1971) by reacting pyruvate or α-ketoisovalerate with $NaBD_3CN$ in the presence of ammonia. The concentration of deuterated amino acid solutions was determined using a Carlo Erba amino acid analyzer. The use of DL mixtures of the substrates was found to have no adverse effect on the reactions with Tv-DAAO and Rg-DAAO (Pollegioni *et al.*, 1992a).

Rapid reaction measurements and turnover experiments were carried out in a thermostated stopped-flow spectrophotometer equipped with a diode array detector (Langkau, 1992) and interfaced with a MacIntosh computer using a POSMA data acquisition and manipulation program (Spectroscopy Instruments GmbH W-8031 Gilching). This program operates in a "fast access mode" which has an acquisition time of 1.8 ms/spectrum with a resolution of 5 nm (1 pixel each 5 nm) and in a "normal access mode" with an acquisition time of 10 ms/spectrum and with a resolution of 0.5 nm (2 pixels/nm). Rapid reactions were routinely recorded in the range 300–650 nm using the normal mode unless specified. The buffer used in experiments with Rg-DAAO was 60/70 mM sodium pyrophosphate, pH 8.5, containing 1.5% glycerol, 0.3 mM EDTA, and 0.75 mM 2-mercaptoethanol (buffer R), and that used with Tv-DAAO was 100 mM Tris-HCl, pH 8.3 (buffer T). In anaerobic experiments the final solution contained 200 mM glucose, 1 × 10^{-7} M glucose oxidase, and 3 × 10^{-8} M catalase; anaerobiosis was obtained by repeated cycles of evacuation and flushing with O_2-free argon. For the experiments involving the oxidation of reduced enzyme, the oxidized form was reacted with a 2.5-fold excess of D-alanine alone (free reduced DAAO) or of the same in the presence of 400 mM ammonium chloride and 20 mM pyruvate (reduced DAAO·IA complex). In the case of Tv-DAAO, we were unable to obtain the free reduced form due to (light induced) formation of radical anion. All concentrations indicated in the context of stopped-flow experiments are those of the reagent after mixing, *i.e.* 1:1 dilution.

Data analysis and fitting of kinetic traces was done on a IBM PS2/386 computer using the "A" program (from D. Ballou, University of Michigan); data representation was done using either the Enzfitter (Elsevier-Biosoft) or DeltaGraph (Delta Point) programs.

RESULTS

Steady State Turnover Kinetics

D-Valine—Oxidized Tv-DAAO was mixed aerobically with excess [2-^{1}H]D-valine in the stopped-flow instrument, and the reaction was followed by continuously recording the absorption spectra in the range 300–650 nm. A rapid, partial decrease of the oxidized flavin absorption was first observed, which was followed by a steady state phase lasting for several seconds and then by a further decrease to reach the final state. This is exemplified in Fig. 1 in which the time course of the 454-nm absorption (the A_{max} for the oxidized enzyme in the visible) is depicted. Subsequent to the first, fast decrease of absorbance, and at the onset of steady state the traces show that the enzyme is present largely in the oxidized form (92% with [2-^{1}H]valine and 96% with [2-^{2}H]valine), indicating that the overall process of reoxidation of reduced DAAO with oxygen is faster than the processes involving reduction. The corresponding values for Rg-DAAO were 96 and 99% with [2-^{1}H]valine and [2-^{2}H]valine, respectively.

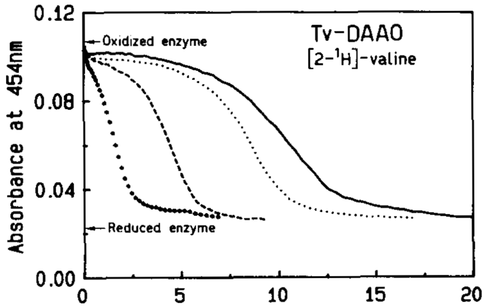

FIG. 1. **Turnover of *T. variabilis* DAAO with D-valine using the stopped-flow instrument.** The enzyme, 5.18 μM, was reacted with 10 mM (• • • •), 5 mM (- - - -), 2.5 mM (· · · ·), and 0.5 mM (——) D-valine (all final concentrations) in buffer T and 25 °C at an initial [O_2] of 253 μM. The course of reaction was monitored by following the absorbance of the oxidized enzyme at 454 nm with time. The *arrows* indicate the absorbance of the enzyme at the beginning and at the end of reaction.

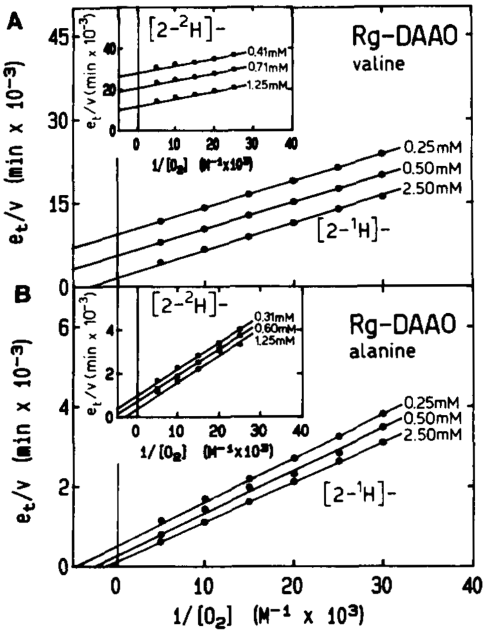

FIG. 2. *A*, Lineweaver-Burk plots of data such as those of Fig. 1, obtained as described in Gibson *et al.* (1964) using *R. gracilis* DAAO (4.5 μM final concentration) with D-valine at the concentration shown and in buffer R at 25 °C. Only a selection of the experimental points is shown; the fitting was linear in the 5–90 *abscissa* value range (0.2–0.011 mM O_2 concentration). The *inset* shows the results obtained using [2-^{2}H]valine as substrate. *B*, same as *A*, however, using [2-^{1}H] alanine and [2-^{2}H]alanine (*inset*) as substrate.

The analysis of these traces in the four sets of experiments was done according to the method of Gibson *et al.* (1964), where the kinetic traces are a record of the rate of catalysis as a continuous function of oxygen concentration. A set of parallel lines was obtained with D-valine as shown in Fig. 2*A* for the Rg-DAAO, and in the insert for the deuterated substrate. Replot of the ordinate intercepts as a function of [2-^{1}H] and [2-^{2}H]D-valine concentration (Gibson *et al.*, 1964) yields lines converging on the negative abscissa for both enzymes (Fig. 3, *A* and *B*), and from the intercepts the K_S and the ϕ_0 values were estimated as reported in Table I. Note that the large kinetic isotope effect on turnover is compatible with the rate-limiting step being in the reductive half-reaction. The K_S and the K_{O_2} values have been determined from both the turnover coefficients ratio and the secondary plots of the turnover rates.

D-*Alanine*—The same steady state experiments as above were carried out with Rg-DAAO and Tv-DAAO using [2-^{1}H] and [2-^{2}H]alanine as substrates. The primary plots also yield parallel line patterns of e_t/v *versus* 1/[O$_2$] as shown in Fig. 2*B*. In contrast to valine as substrate, however, the secondary plots of the ordinate intercepts are not convergent for both enzymes (Fig. 4). The kinetic parameters K_S and K_{O_2} are given in Table I. The large values of K_{O_2} are in good agreement with those previously determined using the polarographic assay for the Rg-DAAO (Pollegioni *et al.*, 1992a).

Spectral Characterization of T. variabilis DAAO

While the spectral properties of PK-DAAO and of Rg-DAAO have been amply documented previously (Porter *et al.*, 1977; Curti *et al.*, 1992; Pilone *et al.*, 1989a) those of Tv-DAAO have not. Fig. 5 shows the spectrum of the oxidized, radical-anion and fully reduced forms of the latter enzyme. The spectra of the oxidized and fully reduced forms are only marginally different from those of the other two enzymes, note *e.g.* the higher resolution of the two main bands centered at 380 and 455 nm, which suggests a more hydrophobic environment (Müller *et al.*, 1973). A major difference was found in the formation of the (red) anionic radical, which, in the case of Tv-DAAO appears to be formed about quantitatively under the conditions of Fig. 5, *i.e.* in the presence of light from reduced enzyme and IA or ketoacid products. The same radical was obtained with PK-DAAO starting from the oxidized enzyme by anaerobic photoreaction in the presence of EDTA (Massey and Palmer, 1966). Under turnover conditions Tv-DAAO can form significant amounts of this radical, and this process is enhanced in the presence of the light. Thus, when reaction courses were monitored in stopped-flow experiments for times exceeding a couple of seconds, control experiments were carried out in parallel in which the light source was turned on and off at regular intervals (not shown) to assess the effect of light on the interconversion of the species shown in Fig. 5.

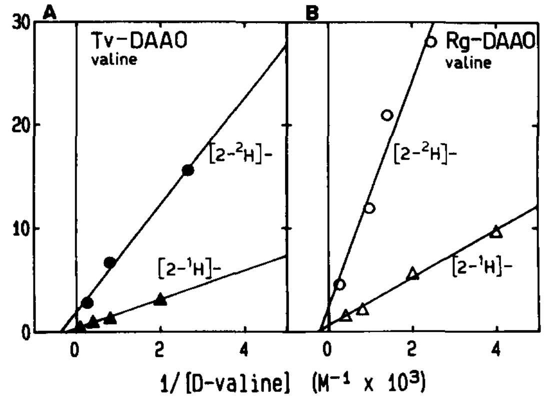

FIG. 3. *A*, secondary plots of the ordinate intercepts from plots of the steady state turnover experiments such as those in Fig. 2*A* using [2-^{1}H]valine (▲) and [2-^{2}H]valine (●) as substrate and *T. variabilis* DAAO. *B*, same as *A*, however, for the *R. gracilis* DAAO and using [2-^{1}H]valine (△) and [2-^{2}H]valine (○) as substrate.

The Reductive Half-reaction

One of the most typical features of PK-DAAO is the reaction with substrate to form colored species having an absorbance beyond 600 nm (Massey and Gibson, 1964), the so called "purple intermediate" (Yagi *et al.*, 1967), which is due to a charge-transfer interaction within the reduced enzyme-IA complex (Massey and Ghisla, 1974). In this respect the two yeast enzymes behave very differently from PK-DAAO as shown in Fig. 6 for Rg-DAAO. This enzyme is reduced rapidly by D-alanine and D-valine at 25 °C and pH 8.5 to yield the typical spectrum of the uncomplexed, reduced enzyme (Pilone Simonetta *et al.*, 1989a). The course of the reaction is clearly biphasic for both enzymes (Fig. 6*B* for Rg-DAAO). A long wavelength absorption, which is indicative of the DAAO$_{red}$-IA charge-transfer complex mentioned above, can be observed transiently and with a very low intensity (see intermediate

TABLE I

Specific steady state coefficients for D-amino acid oxidase from R. gracilis and T. variabilis with valine and alanine in their 2-^{1}H and 2-^{2}H forms as substrates

		Turnover rates and coefficients							
		ϕ_O^{-1}	ϕ_S^{-1} (Expressed)	ϕ_S^{-1} (Calculated)[a]	$\phi_{O_2}^{-1}$	K_S (Expressed)	K_S (Calculated ($\approx(k_{-1}+k_2)/k_1$))	K_{O_2} (Expressed)	K_{O_2} (Calculated (k_2/k_3))[b]
		min^{-1}	*M*$^{-1}$ *min*$^{-1}$			*mM*			
R. gracilis									
Alanine	(H)	20,700	8.0×10^6	($\approx k_1$)	9.0×10^6	2.6	2.6	2.3	3.0
	(D)	4,250	4.2×10^6	6.7×10^6	8.5×10^6	1.0	1.0	0.5	0.6
Isotope effect (H/D)		4.9	1.9		1.06	2.6	2.6	4.6	5.0
Valine	(H)	1,730	4.4×10^5	4.8×10^5	2.2×10^6	3.9	3.8	0.8	0.7
	(D)	360	1.0×10^5	1.3×10^5	3.1×10^6	3.6	2.2	0.12	0.13
Isotope effect (H/D)		6.6	4.4		0.7	1.1	1.7	6.6	5.0
T. variabilis									
Alanine	(H)	3,150	7.7×10^5	($\approx k_1$)	3.8×10^6	4.1	4.5	0.8	1.8
	(D)	440	5.2×10^5	8.8×10^5	2.8×10^6	0.85	0.7	0.16	0.18
Isotope effect (H/D)		7.2	1.5		1.4	4.8	6.4	5.2	10
Valine	(H)	2,500	8.0×10^5	8.5×10^5	3.6×10^6	3.1	2.9	0.7	1.3
	(D)	520	1.9×10^5	2.8×10^5	3.0×10^6	2.7	1.6	0.17	0.25
Isotope effect (H/D)		4.8	4.2		1.2	1.1	1.8	4.1	5.2
Pig kidney									
Alanine[c]	(H)	600 ($\approx k_5$)	4.1×10^5	($\approx k_1$)	8.40×10^6 ($\approx k_3$)	2.0		0.15	

[a] Calculated using k_{red} and K_{dA} values from single turnover experiments as discussed in the text (see legend of Table II for more details).

[b] In the case of Rg-DAAO and valine, k_{ox} is taken as the rate of reoxidation of uncomplexed enzyme.

[c] Yagi *et al.*, 1973.

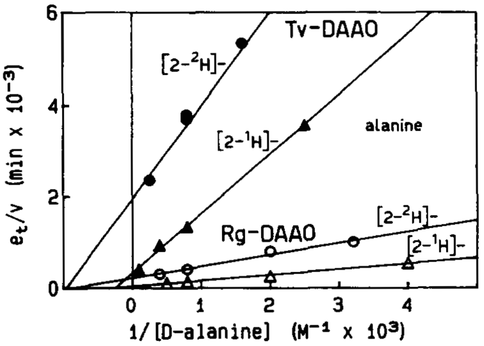

FIG. 4. **Secondary plots of the *ordinate* intercepts form plots of the steady state turnover such as those in Fig. 2*B* using [2-^{1}H]alanine (*triangles*) and [2-^{2}H]alanine (*circles*) as substrate and *R. gracilis* (*open symbols*) and *T. variabilis* (*filled symbols*) DAAOs.**

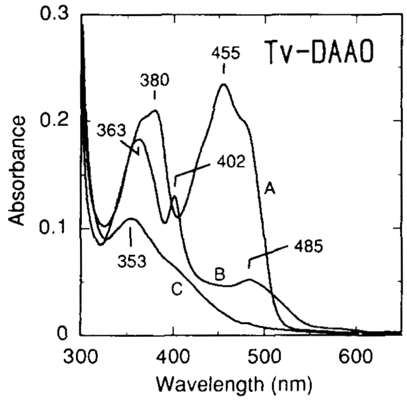

FIG. 5. **Absorbance spectra of *T. variabilis* DAAO 21.7 μM in buffer T, in the oxidized (*A*), radical (*B*), and fully reduced state (*C*) at 25 °C.** Full reduction was achieved upon anaerobiosis and addition of 1 mM DL-alanine (final concentration), and the red radical production upon illumination of the reduced enzyme for 195 min (250-watt halogen lamp at a distance of 11 cm).

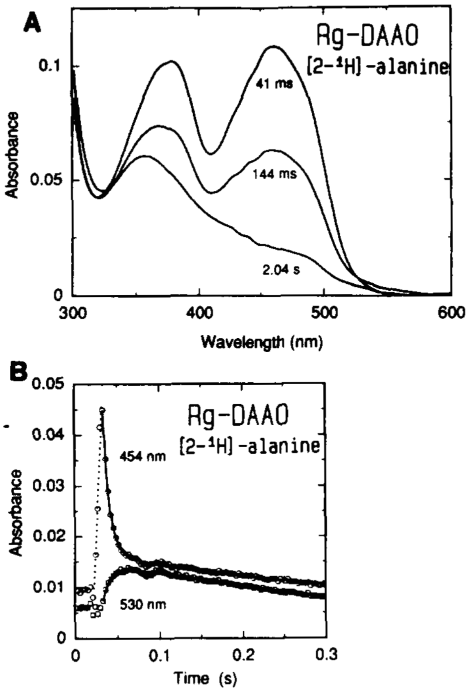

FIG. 6. *A*, time course of anaerobic reduction of *R. gracilis* DAAO using D-alanine, followed by a stopped-flow instrument, and monitored by a diode array photometer. Enzyme, 6.5 μM final concentration, was made anaerobic in buffer R at 25 °C and in the presence of glucose/glucose oxidase and 3×10^{-8} M catalase. The first spectrum shown after mixing with 0.05 mM D-alanine (final concentration) and recorded at 41 ms, is that of essentially unreacted enzyme and corresponds to the point in time at which mixing is complete. The spectrum recorded at 144 ms shows an absorbance extending up to ≈550 nm, which corresponds to partial formation of the transient reduced enzyme complex with α-iminopyruvic acid. At $t > 2$ s, the reaction is essentially complete, and the spectrum recorded at 2.05 s corresponds to that of fully reduced, uncomplexed enzyme. Note that the noise at 430–450 nm is due to a spectrophotometer artifact and that the optical path is 20 mm. *B*, time course of the anaerobic reduction of *R. gracilis* DAAO using 2 mM D-alanine (final concentration) followed at two different wavelengths. At 454 nm the trace reflects the conversion of oxidized to fully reduced enzyme; at 530 nm the formation of reduced enzyme-product complex. The *points* represent single data values and the *full lines* the best fit obtained for two exponential, consecutive decay processes (the data points in the early, mixing phase corresponding to the increasing segment of the curve (- - - -) were not used for the fit). Note that the substrate concentrations in *A* and *B* are different; the traces were obtained using the spectrophotometer fast access mode.

spectrum in Fig. 6, *A* and *B*). Note that with PK-DAAO (Porter *et al.*, 1977), and also with lactate oxidase (Lockridge *et al.*, 1972; Ghisla and Massey, 1991), the comparable intermediate species are easily observed. In the present case, the formation of the IA charge-transfer complex is best observed when the reaction course is monitored at 530 nm using very high substrate concentrations (Fig. 6*B*). Taking the $\epsilon_{530} \approx$ 1,800 $\mathrm{M^{-1}\,cm^{-1}}$, which was estimated from Fig. 8 (see below), it appears that the formation of the $E_{\mathrm{red}}\cdot$IA complex is almost quantitative. Note that as with PK-DAAO (Massey and Gibson, 1964) and lactate oxidase (Lockridge *et al.*, 1972) the rate of decrease of the 454 nm absorption, which reflects DAAO$_{\mathrm{ox}}$ reduction, correlates with the increase at 530 nm. This behavior can be observed also with Tv-DAAO (not shown) with which intermediate formation is even less pronounced spectrally. There, the course of the reaction shows similar rates at 454 nm (decrease), 402 nm (decrease), and at 530 nm (increase). This clearly demonstrates that the anion radical species does not occur at relevant concentrations during the reaction. However, at times >1 s, the absorbance at 402 nm will start to increase due to photochemical processes as mentioned above (not shown). Curves such as those of Fig. 6*B* are biphasic and were best fitted by two exponentials. According to Strickland *et al.* (1975) and as discussed by Fitzpatrick and Massey (1982), when substrate binding (steps k_1, k_{-1}, Equation 2) is relatively small as compared to reduction (k_2) a "lag" on the onset of reduction might be observed. In our case no such effect was observed, the instrument used having a "deadtime" of 3–4 ms (Raichle, 1981).

Thus, the reductive half-reaction can be defined by the following minimal equation (Equation 2):

$$\mathrm{DAAO_{ox} + AA} \underset{k_{-1}}{\overset{k_1}{\leftrightarrow}} \mathrm{DAAO_{ox}\cdot AA} \underset{k_{-2}}{\overset{k_2}{\leftrightarrow}} \mathrm{DAAO_{red}} \cdot \mathrm{IA} \underset{k_{-3}}{\overset{k_3}{\leftrightarrow}} \mathrm{DAAO_{red} + IA} \qquad \text{(Eq. 2)}$$

where DAAO$_{\mathrm{ox}}$ and DAAO$_{\mathrm{red}}$ are the oxidized and the reduced enzyme forms. That $k_2 >> k_{-2}$ is indicated by the extent of the reduction phase measured at 454 nm and at all substrate concentrations, which corresponds approximately to the difference in absorption between DAAO$_{\mathrm{ox}}$ and DAAO$_{\mathrm{red}}$ at this wavelength. In addition, the pattern emerging from the analysis of the primary traces is consistent with a very small rate of step k_{-2}, as discussed by Schopfer *et al.* (1988). The third argument in favor of $k_2 >> k_{-2}$ comes from the results of the anaerobic titration of reduced enzyme with IA, where even at the highest concentrations no formation of oxidized form was detectable. The internal equilibrium governed by k_2/k_{-2} appears thus to lie far to the right, as also is the case with PK-DAAO (Massey and Gibson, 1964; Porter *et al.*, 1977), indicating that the ratio of the redox potentials of the two couples (bound Fl_{ox}/Fl_{red} and AA/IA) must be similar in all three DAAOs.

The step(s) k_1 (and k_{-1}) do not appear to be observable spectrophotometrically. The first fast phase discussed above, *i.e.* that corresponding to the disappearance of the absorbance of $DAAO_{ox}$, would thus reflect k_2 (or $k_1 \cdot k_2$, when $k_{-1} << k_2$) which leads to the transient $DAAO_{red} \cdot IA$ complex (absorbance increase at 530 nm). The second, slower phase, which has similar rates when observed at 454 and at 530 nm (Fig. 6*B*), is ascribed to k_3, *i.e.* to the dissociation of the products iminoacid (or α-keto acid and NH_4^+ from the $DAAO_{red} \cdot IA$ complex.

Fig. 7, *A* and *B* represent the double-reciprocal plots of the rates of the fast phase of reduction for Rg-DAAO at the concentrations of [2-^{1}H] and [2-^{2}H]D-alanine as well as of [2-^{1}H] and [2-^{2}H]D-valine shown. The extrapolated rates for Rg- and Tv-DAAOs are listed in Table II. The line patterns obtained with D-alanine are almost parallel (Fig. 7*A*). This contrasts to what is obtained with D-valine and is shown in Fig. 7*B*. Regression curves in double-reciprocal plots for protio and deutero substrates not extrapolating to the same *abscissa* intercept (*i.e.* to different apparent "K_d" values) have been noted in some cases (Massey *et al.*, 1976; Porter *et al.*, 1977), and its interpretation has caused some difficulties. Fitzpatrick and Massey (1982) have provided a convincing analysis and have shown that this behavior can occur when $k_{-1} \leq k_2 >> k_{-2}$. This seems to be the case with alanine, while for valine the coincidence of the *abscissa* intercepts for the protio and deutero forms suggests a situation where $k_{-1} > k_2$, *i.e.* where true preequilibrium conditions exist. This observation is analogous to that reported by Porter *et al.* (1977) and Yagi *et al.* (1970) for PK-DAAO and should be compared with the analysis of the steady state results shown in Fig. 2, *A* and *B*. In Table II the deuterium isotope effects obtained from data of Fig. 7, *A* and *B*, are also listed.

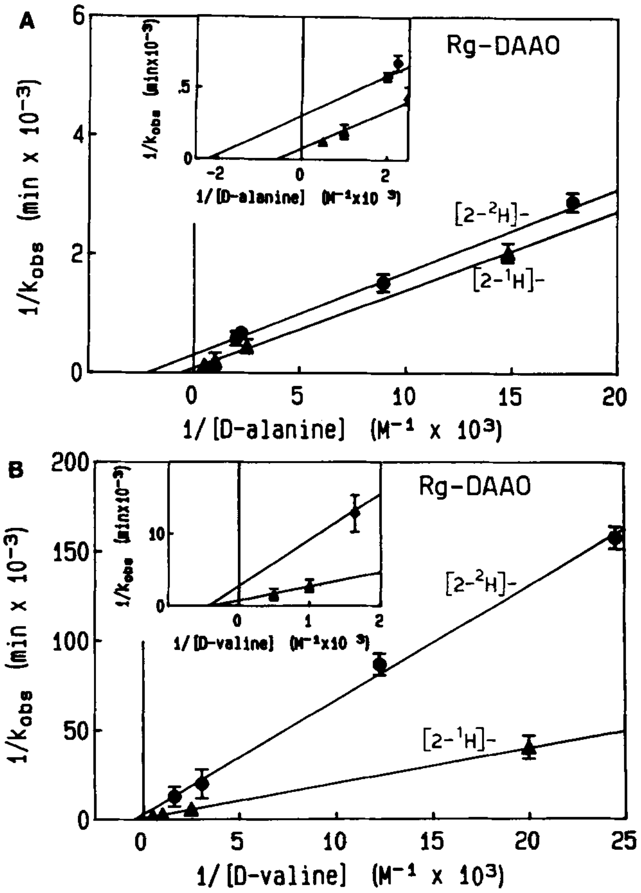

FIG. 7. **Double-reciprocal plots of the data monitored for the anaerobic reductive half-reaction of *R. gracilis* DAAO using protio and deuterated substrates as those shown in Fig. 6, *A* and *B*.** *A*, enzyme in buffer R was mixed anaerobically with [2-^{1}H]alanine (▲) and [2-^{2}H]alanine (●) as substrates. The *inset* shows the *axis* intercepts on an expanded scale. *B*, same as in *A* with [2-^{1}H] valine (▲) and [2-^{2}H]valine (●) as substrates. The *inset* shows the *axis* intercepts on an expanded scale. *Vertical bars*, in both *panels* indicate ±S.E. for six to eight determinations.

The Oxidative Half-reaction

The oxygen reactions of reduced Tv-DAAO and Rg-DAAO in their IA-complexed forms and of free reduced Rg-DAAO are monophasic (not shown) and yield the rates reported in Table II. The uncomplexed form of reduced Tv-DAAO was not obtained due to formation of the radical anion (*cf.* above). Importantly the rates observed with free $Rg\text{-}DAAO_{red}$ were much slower compared to those of the $Rg\text{-}DAAO_{red} \cdot IA$. Two types of reactions may be assumed as shown by the Equation 3a as opposed to Equations 3b and c:

$$DAAO_{red} + O_2 \rightarrow DAAO_{ox} + H_2O_2 \qquad \text{(Eq. 3a)}$$

$$DAAO_{red} \cdot IA + O_2 \rightarrow DAAO_{ox} \cdot IA + H_2O_2 \qquad \text{(Eq. 3b)}$$

$$DAAO_{ox} \cdot IA \rightarrow DAAO_{ox} + IA \qquad \text{(Eq. 3c)}$$

The rate of O_2 reaction of free reduced $Rg\text{-}DAAO_{red}$ (Equation 3a) is clearly inconsistent with the rates of turnover either previously determined with the oxygen electrode (Pollegioni *et al.*, 1992a) or by enzyme monitored turnover (see Table I). This indicates that in turnover another species, and most probably the $DAAO_{red} \cdot IA$ complex, reacts with O_2 according to Equation 3b. While this would correspond to what is observed with PK-DAAO, the observation of only very small absorbancies attributable to the reduced DAAO·IA complexes (*cf.* Fig. 6) indicates that their properties must be significantly different. We have thus attempted the preparation of these complexes by titrating the reduced enzymes with pyruvate in the presence of a large excess of NH_4^+. Indeed complexes are formed which can be detected spectrophotometrically; they have, however, very low extinctions at the low energy side of the main flavin absorption band (Fig. 8). The constants K_d estimated for binding of the IA to reduced Rg-DAAO and Tv-DAAO, as determined by anaerobic titration, were 4 and 2 mM, respectively, and thus of the order found for binding to PK-DAAO (Massey and Gibson, 1964; Fitzpatrick and Massey, 1982). This confirms that the employed concentration of IA was sufficient to ensure essentially complete $E_{red} \cdot IA$ complex formation in the oxidation experiments referred to above.

The primary data obtained from reoxidation experiments can be analyzed assuming a second order processes. In linear plots of the primary data (not shown), no indication for saturation with O_2 can be seen, and with uncomplexed $Rg\text{-}DAAO_{red}$ there is no discernible *y* axis intercept. With the $DAAO_{red} \cdot IA$ complexes of both enzymes, the curve extrapolation to a *y* -axis intercept is quite clear cut and particularly so with Tv-DAAO. This is compatible with a reversible second order process for the oxygen reaction and allows the estimation of its reversal (k_{-3}, *cf.* Table II). From a chemical point of view and also in comparison with most oxidases (Ghisla and Massey, 1989), a direct reaction with O_2 is assumed to be quite reasonable.

DISCUSSION

The comparison of the spectral properties of Rg-DAAO and Tv-DAAO (Figs. 5, 6*A*, and 8) at the three different states of oxidation with the corresponding ones of PK-DAAO (Curti *et al.*, 1992) indicates substantial differences at the level at which the flavin cofactor interacts with the protein environment and with the substrate. This appears to be the case in particular in the complex between (enzyme bound) reduced flavin and product. In the case of the related α-OH-acid oxidase (Ghisla and Massey, 1989), the product pyruvate is placed above the flavin plane (Lederer, 1991) where it interacts with the π-orbitals of the latter to yield the typical long wavelength charge transfer transition. Such an interaction is most probably occurring with PK-DAAO, but is likely to be substantially different with the two yeast enzymes. Earlier studies using modified FAD-cofactors are in line with this conclusion (Pollegioni *et al.*, 1992b). These differences might reflect the factors which also influence the rates of product release, which in turn are most different between the yeast and PK-DAAOs. The stabilization of the red anionic radical also suggests differences at the active center.

The cycle catalyzed by Rg-DAAO and Tv-DAAO is consistent with the following kinetic mechanism, which is analogous to that proposed by others for PK-DAAO (Porter *et al.*, 1977; Fitzpatrick and Massey, 1982) (Scheme I):

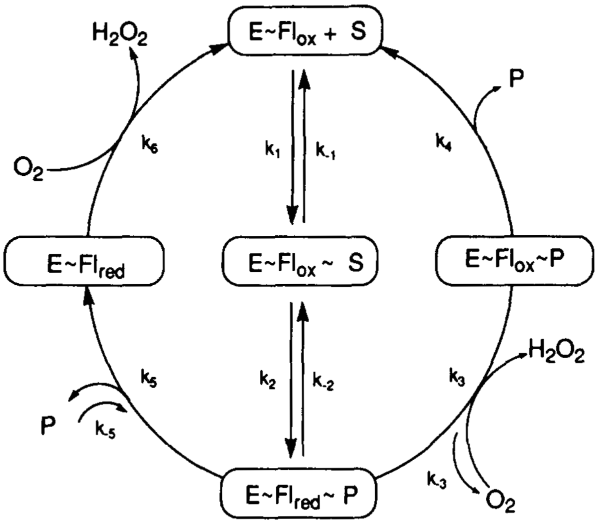

SCHEME I. **Kinetic mechanism proposed for the catalytic cycle of yeast DAAOs.** Note that reduced enzyme species will react reversibly with oxygen via encounter complexes, which have been omitt ed for clarity.

The finding of a parallel line pattern in the secondary plots of Fig. 2, *A* and *B*, is diagnostic of a binary complex mechanism (ping pong) or of a limiting case of a ternary complex mechanism, where some specific rate constants are sufficiently small (Palmer and Massey, 1968; Porter *et al.*, 1977; Fitzpatrick and Massey, 1982). In our case the sequential mechanism represented by the right loop of Scheme I appears to best describe the data, while the involvement of the left hand branch might play only a minor role. When the reductive half-reaction ($k_{red} \approx k_2$) is practically irreversible ($k_2 >> k_{-2}$) a case is given where a parallel pattern in plots such as those of Fig. 2, *A* and *B* can result. This corresponds to the overall kinetic scheme proposed by Palmer and Massey (1968) as also discussed later by Fitzpatrick and Massey (1982).

For this simplified mechanism the steady state is described by Equations 4 and 5:

$$\frac{e_t}{v} = \phi_0 + \frac{\phi_S}{[S]} + \frac{\phi_{O_2}}{[O_2]} + \frac{\phi_{SO_2}}{[S][O_2]} \qquad \text{(Eq. 4)}$$

$$\frac{e_t}{v} = \frac{k_2 + k_4}{k_2 \cdot k_4} + \frac{k_{-1} + k_2}{k_1 \cdot k_2[S]} + \frac{k_2 + k_{-2}}{k_2 \cdot k_3[O_2]} + \frac{k_{-1} \cdot k_{-2}}{k_1 \cdot k_2 \cdot k_3[S][O_2]} \qquad \text{(Eq. 5)}$$

where e_t = [total enzyme] and v = velocity of the reaction,

$$\phi_{zero}^{-1} = V_{max'} \quad \frac{\phi_S}{\phi_{zero}} = K_S \text{ and } \frac{\phi_{O_2}}{\phi_{zero}} = K_{O_2}. \qquad \text{(Eq. 6)}$$

This is the same as that previously shown to apply to the pig kidney enzyme, at least in those cases where a detailed analysis was carried out (Porter *et al.*, 1977; Fitzpatrick and Massey, 1982). However, with the latter enzyme, the term k_4 (Scheme I) which corresponds to product release is important in the reaction, whereas with both yeast enzymes $k_4 >> k_2$.

This simplification appears to be generally valid and follows from $\phi_O^{-1} \approx (k_2.k_4)/(k_2 + k_4)$ and the finding that $\phi_O^{-1} \approx k_2$ (compare Tables I and II). The expression $K_{O_2} = (k_4 \cdot (k_2 + k_{-2}))/(k_3 \cdot (k_2 + k_6))$ can also be simplified to k_2/k_3 and that of $K_s = ((k_4 \cdot (k_{-1} + k_2))/(k_1 \cdot (k_2 + k_4))$ to $(k_{-1} + k_2)/(k_1))$.

A test for the validity of this is to compare the calculated values of K_{O_2} with those observed in steady state turnover. Both are listed in Table I. The correspondence is very good for Rg-DAAO while for Tv-DAAO the discrepancy of the values is up to a factor 2 for the protio substrates, suggesting that in these cases k_4 is comparatively smaller and of the order of k_2. The good correspondence of experimental and calculated values also extends to the deuterium isotope effects which are listed in Table I.

In the case of alanine, the secondary plot of the rates of turnover (Fig. 4) yields a pattern which clearly does not converge on the negative *x* axis, but also is not parallel, *i.e.* has an intermediate character. To a lesser extent this is also the case for the secondary plots of the rapid reduction data shown in Fig. 7*A*. This suggests an intermediate situation where $k_{-1} \leq k_2$. In the clear cut case of $k_{-1} << k_2$ ($\phi_{Ala^{-1}} = k_1$) parallel lines would be expected along with identical ϕ_S^{-1} values for both protio- and deutero-alanine (*i.e.* no isotope effect on the slope of the plot). It thus appears that $\phi_{Ala^{-1}}$ is probably close to k_1 but that k_{-1} also approaches the value of k_2, in particular with [2-^{2}H]alanine; in this latter case we would have $k_{-1} \approx k_2$, and therefore $\phi_{S^{-1}} \approx (k_1)/(2)$. The validity of these assumptions is supported by the good correspondence of calculated and experimental values of K_s (Table I).

The third and fourth terms can be assumed to be $\phi_{O_2^{-1}} = (k_2 \cdot k_3)/(k_2 + k_{-2}) \approx k_3$, and $\phi_{SO2}^{-1} \approx 0$ since k_{-2} indeed should be negligible, again in agreement with the finding of parallel lines in plots such as those of Fig. 2, *A* and *B*. The actual velocity of the Rg-DAAO$_{red}$·IA complex reaction with O_2 is higher than that of (uncomplexed) Rg-DAAO$_{red}$, consistent with turnover also proceeding via the ternary complex.

The same probably holds also for Tv-DAAO since the rate of O_2 reaction of the Tv-DAAO$_{red}$·IA complex is similar to $\phi_{O_2^{-1}}$ (Tables I and II). These deductions are in line with the behavior of Rg-DAAO and Tv-DAAO in enzyme-monitored turnover assays as depicted by the *traces* shown Fig. 1. There, at the onset of turnover, the relative absorptions of starting enzyme and of turnover state reflect the ratio of the reductive as compared to the oxidative half-reactions. On the other hand, it is conceivable that at least with Tv-DAAO and at low O_2 concentration some percent of the oxidative half-

TABLE II

Specific rate constants obtained from stopped-flow experiments for D*-amino-acid oxidase from R. gracilis and T. variabilis and for with valine and alanine in their* 2-^1H *and* 2-^2H *forms as substrate*

K_d is the abscissae extrapolation in double-reciprocal plots of measured rates *versus* substrate concentration. In the case of alanine, and as discussed in the text this value does not reflect k_{-1}/k_1. k_{red} is the rate of the fast and, from the point of view of the extent, major phase of enzyme reduction measured at 454 nm, as obtained from fits of primary kinetic traces. k_{diss} is the second, slow phase of minor extent, which follows the first phase of absorbance decrease at 454 nm and absorbance increase at 530 nm, and corresponds to product dissociation from the reduced enzyme-imino acid complex (*cf.* Fig. 6*B*). k_{ox} is the rate of O_2 reaction of the species shown as followed by the appearance of the spectrum of the oxidized flavin.

		Turnover rates and coefficients							
		Reductive half-reaction						Oxidative half-reaction	
		K_d $(\approx(k_2 + k_{-1})/k_1)$	k_{red} $(\approx k_2)$	Calculated		Slope $((k_2 \cdot k_{-1})/(k_2 + k_{-1}))$	k_{diss} $(\approx k_5)$	$k_{\mathrm{off}(O_2)}$ $(\approx k_{-3})$	$k_{\mathrm{on}(O_2)}$ $(\approx k_3$ or $k_6)$
				k_1	k_{-1}				
		mM	min^{-1}	$M^{-1}\,min^{-1}$	min^{-1}	$M^{-1}\,min^{-1}$	min^{-1}	min^{-1}	$M^{-1}\,min^{-1}$
R. gracilis									
Alanine	(H)	2.8	20,100	1.0×10^7	5,830	7.2×10^6	165		
	(D)	0.6	4,000			7.1×10^6	130		
Isotope effect (H/D)			5.0						
Valine	(H)	3.8	1,820	9.1×10^5	1,675	4.7×10^5	71		
	(D)	2.6	350			1.6×10^6	8.3		
Isotope effect (H/D)			5.2						
$E_{\mathrm{red}} \sim \mathrm{P} + \mathrm{O}_2$[a]								70	(k_3) 6.8×10^6
$E_{\mathrm{red}} + \mathrm{O}_2$									(k_6) 2.8×10^6
T. variabilis									
Alanine	(H)	3.4	3,475	8.1×10^5	200	7.9×10^5	218		
	(D)	0.4	350			7.9×10^5	85		
Isotope effect (H/D)			9.9						
Valine	(H)	2.9	2,460	1.5×10^6	1,900	8.4×10^5	210		
	(D)	1.7	480			1.7×10^5	17		
Isotope effect (H/D)			5.1						
$E_{\mathrm{red}} \sim \mathrm{P} + \mathrm{O}_2$[a]								40	(k_3) 1.9×10^6
Pig kidney									
Alanine[b]	(H)	420	240,000	6.0×10^5	11,100[c]		1.0		
	(D)	110	60,000						
Isotope effect (H/D)		3.8	4.0 (1.15)[d]						
Valine[e]	(H)	2.9	2,100						
	(D)	2.9	750						
Isotope effect	(H/D)	1.0	2.8						
$E_{\mathrm{red}} \sim \mathrm{P} + \mathrm{O}_2$[b]								(k_4) 600	(k_3) 1.0×10^7
$E_{\mathrm{red}} + \mathrm{O}_2$[b]									(k_6) 2.8×10^6

[a] $E_{\mathrm{red}} \sim \mathrm{P}$ stands for the complex of reduced enzyme and the product from alanine, *i.e.* iminopyruvate.
[b] Porter *et al.*, 1977.
[c] Fitzpatrick and Massey, 1982.
[d] Denu and Fitzpatrick, 1992.
[e] Yagi *et al.*, 1973.

reaction proceeds via the alternate pathway of steps $k_5 + k_6$ (*cf.* left loop of Scheme I).

The isotope effects found on the reduction half-reaction (Table II) are likely to be close to the intrinsic ones; their magnitude is higher or comparable to that found by Denu and Fitzpatrick (1992) for alanine and serine. The differences in rates of k_{diss} (Table II) depending on α-deuteration of the amino acid substrate most likely has no specific meaning. The experimental error in particular with Tv-DAAO was large due to the small amplitude of the observable spectral changes and the fact that the resolution of the phases connected with enzyme reduction is probably not complete.

In the case of Rg-DAAO and D-alanine as substrate, we have observed no effect of enzyme concentration on turnover results, in all cases parallel lines were observed. This suggests that with the yeast enzyme polimerization equilibria are not relevant under the experimental conditions used. However, with D-valine as substrate there is a substantial ~18-fold difference in turnover rates between the polarographic assays, pH 8.5 and 30 °C (Pollegioni *et al.*, 1992a), and the enzyme monitored assays reported here (pH 8.5 and 25 °C), which probably can only in part be ascribed to the effect due to different temperatures. This aspect is currently under investigation.

Taken together, the rapid kinetics results for the two yeast DAAOs are consistent with an ordered sequential mechanism where the rate of reduced intermediate production parallels the turnover number and is mainly rate limiting for the overall catalytic process. The higher catalytic efficiency of yeast DAAOs compared to the mammalian enzyme thus results from a much higher rate of dissociation of product from the $\mathrm{DAAO_{ox}}\cdot\mathrm{IA}$ complex, which leads to a different location of the rate-limiting step. This raises the question about the ultimate reason for which mammalian DAAO have evolved to control catalysis via product release. In some yeasts, as described for *R. gracilis* (Pilone Simonetta *et al.*, 1989b), DAAO is induced to a high level of expression by the presence of D-amino acids in the growth medium, when these compounds represent the only source of nitrogen and/or carbon for the organisms, and this might have constituted the biological and evolutionary drive to obtain a higher catalytic efficiency at the expense of control.

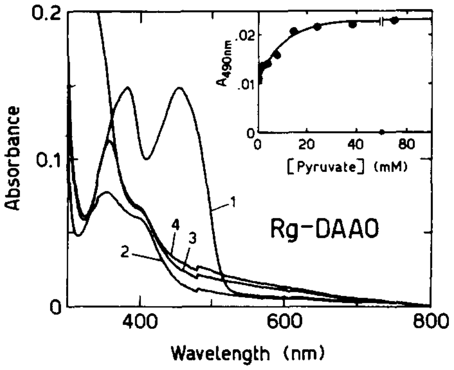

FIG. 8. **Absorption spectra of reduced *R. gracilis* DAAO complexed with iminopyruvate.** The oxidized enzyme, 11.7 μM in buffer R containing 4×10^{-8} M catalase (*curve 1*) was converted anaerobically to the fully reduced species by addition of 5×10^{-4} M D-alanine in the presence of 400 mM ammonium chloride (*curve 2*). The concentrations of added pyruvate are shown in the *inset*. *Curve 4* corresponds to the complex in the presence of 83 mM pyruvate. Note that the absorbance at <380 nm seen in *curves 3* and *4* is due to the absorbancies of pyruvate and iminopyruvate.

Acknowledgments—We thank Dr. D. Ballou for providing the "A" computer program and valuable discussions, Drs. V. Massey and P. Fitzpatrick for critical comments on the manuscript, and Dr. S. Butò and F. Ceciliani for performing synthesis and analysis of deuterated substrates.

REFERENCES

Borch, R. F., Bernstein, M. D., and Dupont Durst, H. (1971) *J. Am. Chem. Soc.* **93,** 2897–2904

Casalin, P., Pollegioni, L., Curti, B., and Pilone Simonetta, M. (1991) *Eur. J. Biochem.* **197,** 513–517

Curti, B., Ronchi, S., and Pilone Simonetta, M. (1992) in *Chemistry and Biochemistry of Flavoenzymes* (Müller, F., ed) Vol. III, pp. 69–94, CRC Press, Boca Raton

Denu, J. M., and Fitzpatrick, P. F.(1992) *Biochemistry* **31,** 8207–8215

Fitzpatrick, P. F., and Massey, V. (1982) *J. Biol. Chem.* **257,** 12916–12923

Ghisla, S., and Massey, V. (1989) *Eur. J. Biochem.* **181,** 1–17

Ghisla, S., and Massey, V. (1991) in *Chemistry and Biochemistry of Flavoenzymes* (Müller, F., ed) Vol. II, pp. 243–289, CRC Press, Boca Raton

Gibson, Q. H., Swoboda, B. E. P., and Massey, V. (1964) *J. Biol. Chem.* **259,** 3927–3934

Langkau, B. (1992) *Studies with Flavin Coenzymes-Catalytic Mechanism of 2-Amino Benzoyl-CoA Monooxygenase-Reductase and of Yeast* D*-Amino Acid Oxidases.* Ph.D. thesis, University of Konstanz

Lederer, F. (1991) in *Chemistry and Biochemistry of Flavoenzymes* (Müller, F., ed) Vol. II, pp. 153–242, CRC Press, Boca Raton

Lockridge, O., Massey, V., and Sullivan, P. A. (1972) *J. Biol. Chem.* **247,** 8097–8106

Massey, V., and Gibson, Q. H. (1964) *Fed. Proc.* **23,** 18–29

Massey, V., and Ghisla, S. (1974) *Ann. N. Y. Acad. Sci.* **227,** 446–451

Massey, V., and Palmer, G. (1966) *Biochemistry* **5,** 3181–3189

Massey, V., Palmer, G., and Bennet, R. (1961) *Biochim. Biophys. Acta* **48,** 1–9

Massey, V., Ghisla, S., Ballou, D. P., Walsh, C. T., Cheung, Y. T., and Abeles, R. H. (1976) in *Flavins and Flavoproteins* (Singer, T. P., ed) pp. 199–212, Elsevier, Amsterdam

Müller, F., Mayhew, S. G., and Massey, V. (1973) *Biochemistry* **12,** 4654–4660

Palmer, G., and Massey, V. (1968) in *Biological Oxidations* (Singer, T. P., ed) pp. 263–300, John Wiley and Sons, New York

Pilone Simonetta, M., Pollegioni, L., Casalin, P., Ronchi, S., and Curti, B. (1989a) *Eur. J. Biochem.* **180,** 199–204

Pilone Simonetta, M., Verga, R., Fretta, A., and Hanozet, G. M. (1989b) *J. Gen. Microbiol.* **135,** 593–600

Pollegioni, L., and Pilone, M. S. (1992c) *Protein Expression Purif.* **3,** 165–167

Pollegioni, L., Falbo, A., and Pilone, M. S. (1992a) *Biochim. Biophys. Acta* **1120,** 11–16

Pollegioni, L., Ghisla, S., and Pilone, M. S. (1992b) *Biochem. J.* **286,** 389–396

Porter, D. J. T., Voet, J. G., and Bright, H. J. (1977) *J. Biol. Chem.* **252,** 4464–4473

Raichle, P. (1981) *Untersuchungen zum Reaktions Mechanismus der Acyl-CoA Dehydrogenasen.* Ph.D. thesis, University of Konstanz

Schopfer, L. M., Massey, V., Ghisla, S., and Thorpe, C. (1988) *Biochemistry* **27,** 6599–6611

Strickland S., Palmer, G., and Massey, V. (1975) *J. Biol. Chem.* **250,** 4048–4052

Yagi, K., Okamura, K., Naoi, M., Sugiura, N., and Kotaki, A. (1967) *Biochim. Biophys. Acta* **146,** 77–90

Yagi, K., Nishikimi, M., Ohishi, N., and Takai, A. (1970) *FEBS Lett.* **6,** 22–24

Yagi, K., Nishikimi, M., Takai, A., and Ohishi, N. (1973) *Biochim. Biophys. Acta* **321,** 64–71